

# The development of an object-oriented classification model for operational burned area mapping on the Mediterranean island of Thasos using LANDSAT TM images

G.H. Mitri

*Dept. of Environmental Management, Mediterranean Agronomic Institute of Chania, Crete, Greece*  
*Email: gmitri@maich.gr*

I.Z. Gitas

*Dept. of Environmental Management, Mediterranean Agronomic Institute of Chania, Crete, Greece*  
*P.O. Box 85, Chania, Crete, Greece. Email: ioannis@maich.gr*

**Keywords:** object-oriented classification, burned area mapping, operational remote sensing

**ABSTRACT:** Multispectral classification, one of the most commonly used methods for mapping burned areas, is based on the spectral properties of different classes of interest and employs special algorithms designed to perform various types of spectral analysis. However, the use of these classifications has been repeatedly reported to create confusion between burned areas and non-vegetation categories, especially water bodies and shaded areas. As a result of the aforementioned, spectral based classification methods cannot be used operationally for the mapping of burned areas from satellite images. On the other hand, object-oriented image classification, which is based on fuzzy logic, allows the integration of a broad spectrum of different object features, such as spectral values, shape and texture. Sophisticated classification, incorporating contextual and semantic information, can be performed by utilizing not only image object attributes but also the relationship between networked image objects. In this study the synergy of all these features allowed us to address image analysis tasks that, up till now, have not been possible. The aim of this work was to develop an object-oriented classification model for operational burned area mapping on the Mediterranean island of Thasos using LANDSAT TM images. An object-oriented specified model was used to map burned areas in two different Mediterranean areas after the LANDSAT TM images had been radiometrically, geometrically and topographically corrected. The combination of the object-oriented approach and the multispectral resolution data of LANDSAT TM showed very promising results in burned area mapping and in discriminating between burned and the other classes of confusion.

## 1 INTRODUCTION

Forest fires are an integral part of many terrestrial ecosystems such as boreal forest, temperate forests, Mediterranean ecosystems, savannas and grasslands among others. With an average of 50 000 fires and 600 000 ha burned, forest fires in the Mediterranean basin account for a significant percentage of fires occurring worldwide (Alexandrian 1995, Esnault and Calabri 1998).

Although information concerning the location and extent of the fire are important to assess economic losses and ecological effects (Caetano et al. 1994, Pereira et al. 1997), most of the National Forest Services in Mediterranean Europe do not provide cartographic representation of burned areas (Chuvienco 1997). Reliable monitoring and effective analysis techniques need to be implemented in order to estimate the ecological impact of fire on the Mediterranean ecosystems (Gitas 1999).

Remote sensing images not only provide extensive coverage wide areas, but also provide comprehensive information about them. Due to the lack of precise mapping of fire boundaries occurring in many areas, remote sensing has been widely applied to overcome this problem (Diaz-Delgado et al. 1998). The wide coverage and high frequency provided by satellite sensors, as well as the information they provide about non-visible spectral regions, makes them a very valuable tool for the prevention, detection and mapping of wildland fires. Indeed, remotely sensed data can contribute to a better, cost effective, objective and time-saving method to quantify the location, aerial extent and intensity of fire events (Chuvieco 1999). Different satellites have proved to be useful in achieving this, for example, LANDSAT with its Thematic Mapper instrument which provides very impressive color images covering an area of 180x180km with 30m resolution.

Despite the advantages of remote sensing, several problems have been confronted in burned area mapping using satellite data. The use of multispectral classification, one of the most common methods for burned area mapping, has been repeatedly reported to create various types of confusion that can affect the accuracy of mapping, the most important of which can be summarized as follows:

- spectral overlapping between slightly burned areas and other non-vegetation categories, especially water bodies, urban areas and bare soil (Huete et al. 1995, Tanaka et al. 1983, Ponzoni et al. 1986, Parnot 1988, Pereira and Setzer 1993, Lombrana 1995, Siljestrom and Moreno 1995, Silva 1996, Caetano et al. 1996);
- spectral overlapping between burned areas and shaded unburned areas (Caetano et al. 1994, Pereira et al. 1997);
- spectral overlapping between surface burned areas and unburned forest (Chuvieco and Congalton 1988, Simpson 1990).

As a result of the above, spectral based classification methods cannot be used operationally for mapping burned areas from remotely sensed data. Object-oriented classification is based on fuzzy logic to allow the integration of a broad spectrum of different object features such as spectral values, shape, texture and contextual information.

The main objective of this work was to develop an object-oriented classification model for operational burned area mapping on the Mediterranean island of Thasos using LANDSAT TM images. The specific objectives were:

- to develop an object-oriented model for burned area mapping using LANDSAT TM images;
- to test the accuracy of the model in a different burned area on Thasos island;
- to test whether the developed model is operational and robust enough for burned area mapping by applying it on other image in Spain.

## 2 STUDY AREA AND DATASET

Two study areas were used in this study. The Mediterranean island of Thasos in Greece was used to develop and test the model for burned area mapping, while the area of "Hoya De Bunol" in Spain was used to check whether the model built is operational in a different Mediterranean ecosystem.

Thasos, of volcanic origin, is Greece's most northerly island (Figure 1). Its area is 399 sq. km, while its perimeter is approximately 102 Km; almost circular in shape, it has a length from N to S of 24 km and a width of 19 km, extending from 24°30' to 24°48' East and 40°33' to 40°49' North. The mountain sides are covered with forests, pines, planes, and chestnut trees predominating. Before 1984, forests and forested lands covered 47.5% of the island (Makedos 1987).

The fires that occurred on Thasos island, in 1985 and 1989 were mainly crown fires which caused the destruction of 11870 ha and 9500 ha, respectively, of different landcover types. The geomorphology of the island, the large extent of the 1985 and 1989 fires, the landcover types, as well as the existence of water bodies render the location of the case study an ideal site for operational burned area mapping.

The second study area represents an area called “Hoya de Bunol” in Spain is home to one of the largest fires occurring on the Mediterranean coast of Spain in the last decades. The fire, which took place in the summer of 1991, destroyed more than 18,000 hectares of forest and shrub land. The study area is representative of the typical characteristics of Mediterranean coastal mountains covered mainly by *Pinus Halepensis* and various types of shrubs.

Two LANDSAT TM images showing burns that occurred in 1985 and 1989 were obtained for this study in order to examine the possibility of applying object-oriented image analysis prior to the operational mapping of recently burned areas from LANDSAT TM images. The acquisition dates for the images were the 24<sup>th</sup> September, 1985 and the 19<sup>th</sup> September, 1989, respectively, sensed a few weeks after the two fires had burned out. Another LANDSAT TM image showing burns that occurred in Bunol, Spain was also obtained for this study. The acquisition date for the last image was 24<sup>th</sup> August, 1991.

The other datasets used in this study were: a forest service fire perimeter map of the three fires on Thasos and in Spain, a 1:50 000 topographic map of Thasos and a digital elevation model with 10 m pixel size generated from a 1: 5000 contour maps of Thasos.

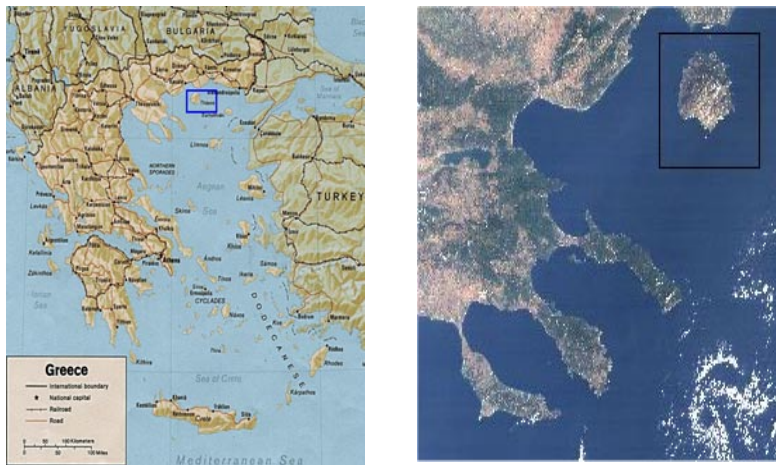


Figure 1. Left: Map of Greece and location of Thasos. Right: Satellite image of Thasos island

### 3 METHODOLOGY

Prior to the object-oriented image analysis the satellite images were pre-processed. Pre-processing of the remotely sensed data (all three TM images) included their atmospheric correction. The LANDSAT images of 1985 and 1989 were corrected geometrically and further corrected for topographic slope and aspect effects, a process most commonly known as topographic normalization.

Subsequently, object-oriented image analysis was applied to the three pre-processed images using the same model for burned area classification developed and tested on the LANDSAT 1985. The results of the three classifications were then assessed for their accuracy, followed by comparisons with the fire perimeters published by the Greek Forest Service and ICONA (Figure 2).

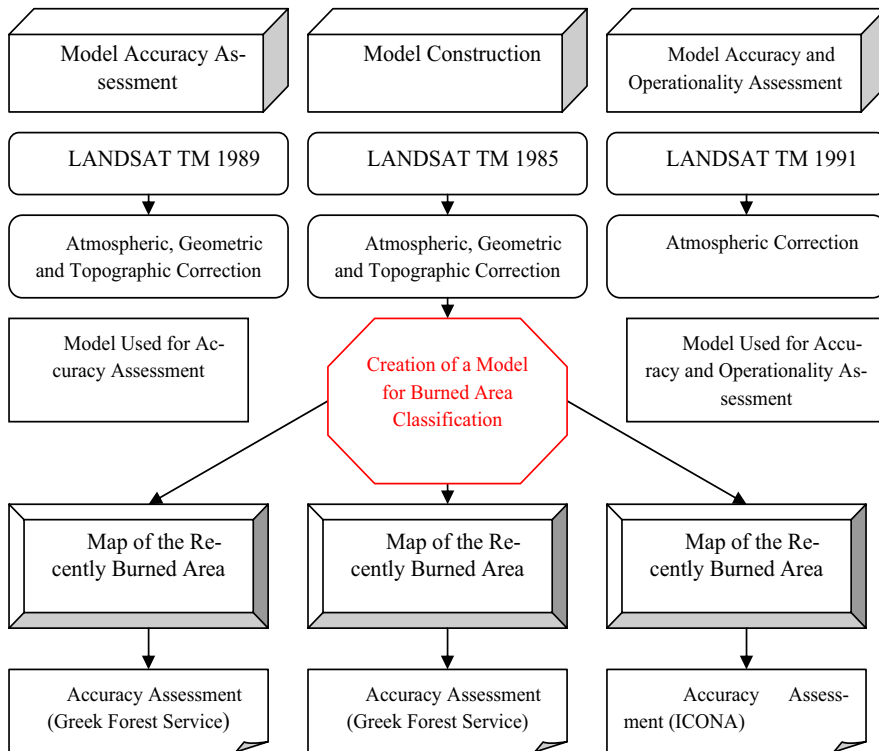


Figure 2. The flowchart of the methodology

### 3.1 Data preprocessing

The three LANDSAT TM images from different dates were pre-processed. The LANDSAT images of 1985 and 1989 were atmospherically, geometrically and topographically corrected, while the LANDSAT of 1991 was only atmospherically corrected.

Preprocessing forms a preparatory phase that, in principle, improves image quality as the basis for later analyses that will extract information from the images. The influence of the atmosphere degradation was removed by the radiometric correction. Geometric correction was made to bring the remotely sensed data into registration with the topographic maps in order to make the images and the auxiliary data geographically comparable. Several studies concerned with burned area mapping using LANDSAT TM have reported confusion between burned areas and topographically shaded areas (Tanaka et al. 1983, Milne 1986, Chuvieco and Congalton 1988, Parnot 1988, Pereira 1992, Caetano et al. 1994, Lombrana 1995, Pereira et al. 1997). Topographic normalization was applied to the LANDSAT TM images from Thasos in order to minimize the confusion.

The Spatially-Adaptive Fast Atmospheric Correction Algorithm (ATCOR2), which was developed by Richter (1997) and compiled using the MODTRAN-2 and the SENSAT-5 codes, was used in this study. The model calculates a ground reflectance image in each spectral band: the first step assumes an isotropic (Lambert) reflectance law, neglecting the neighbourhood of each pixel. The second step accounts for the influence of the neighbouring background (adjacency effect).

The LANDSAT model was used to geometrically correct the two LANDSAT TM images. The LANDSAT model allows ortho-rectification of LANDSAT data, such as TM, which has multiple perspective centers. In the ortho-rectification process, relief displacement was corrected with the use of a DEM by including Z values (elevation from the DEM). Sensor attitude/orientation was

corrected by taking into account the exterior orientation (position and orientation), and internal sensor errors were corrected by looking at the internal geometry of the sensor.

A 10-metre grid size Digital Terrain Model (DTM) and a 1:50 000 planimetric map were used in the process. The geometric correction proceeded by identifying GCPs in the LANDSAT images and on the planimetric map. The two images were then reprojected using a continuous polynomial approximation into the Greek EGSA projection system, a process by which the geometry of the image areas is made planimetric by referring to a standard map projection.

The statistical technique of least squares regression was used to determine the coefficients for the coordinate transformation equations. The total  $RMS_{error}$  associated with the GCPs used for orthorectifying the 1985 and the 1989 LANDSAT images was equal to 0.31 and 0.37, respectively. Without doubt these solutions with low RMS would be good fits for the two datasets.

The De-relief algorithm developed by Costa-Posada (1997) was used in this study. It corrects atmospherically corrected satellite data for the topographic effect using the Minnaert model with a single  $k$  coefficient for every different band of the image. Its use for each band separately makes it possible to correct each band with a different  $k$  coefficient (Gitas 1999).

### 3.2 *Object-oriented model development*

Subsequent to the pre-processing, object-oriented image analysis was applied to the images. The 1985 LANDSAT was first used to develop the object-oriented classification model, which was also tested as well on the two other LANDSAT images.

In contrast to classic image processing methods, the basic processing units of object-oriented image analysis are image objects or segments and not single pixels, moreover, classification acts on image objects. One motivation for the object-oriented approach is the fact that, in many cases, the expected result of most image analysis tasks is the extraction of real world objects, proper in shape and proper in classification. This expectation cannot be fulfilled by traditional, pixel-based approaches (Baatz and Shape 1999).

The concept is that important semantic information necessary to interpret an image is not represented in single pixels, but in meaningful image objects and their mutual relations. Image analysis is based on contiguous, homogeneous image regions that are generated by initial image segmentation. Connecting all the regions, the image content is represented as a network of image objects. These image objects act as the building blocks for the subsequent image analysis. In comparison to pixels, image objects carry much more useful information. Thus, they can be characterized by far more properties such as form, texture, neighborhood or context, than pure spectral or spectral-derivative information (Baatz and Shape 2000).

Analysis of an image in the object-oriented approach involved classifying the image objects according to class descriptions organized in an appropriate knowledge base. The knowledge base itself was created by means of inheritance mechanisms, concepts and methods of fuzzy logic and semantic modeling. The development of the object-oriented model involved two steps, namely segmentation and classification.

#### 3.2.1 *First step: segmentation*

Segmentation is not an aim in itself. As regards the object-oriented approach to image analysis, the image objects resulting from a segmentation procedure are intended to be rather image object primitives, serving as information carriers and building blocks for further classification or other segmentation processes. In this sense, the best segmentation result is the one that provides optimal information for further processing (Hofmann, Puzicha and Buhmann 1998).

The segmentation used in this study was a bottom up region-merging technique starting with one-pixel objects. In numerous subsequent steps smaller image objects are merged into bigger ones. The procedure simulates an even and simultaneous growth of segments over a scene in each step. The algorithm guarantees a regular spatial distribution of treated image objects. The underlying patented algorithm is essentially a heuristic optimization procedure that minimizes the average heterogeneity of image objects for a given resolution over the whole scene. Heterogeneity itself is

based not only on the standard deviation of image objects but also on their shape. Weighting between spectral and shape heterogeneity enables the adjustment of segmentation results to the considered application.

After segmentation, all image objects were automatically linked to a network in which each image object knows its neighbors, thus affording important context information for later analysis. Subsequently, repetition of segmentation with different scale parameter creates a hierarchical network of image objects. Each image object knows its super-object and its sub-objects. Figure 3, shows the concept of segmentation, in which where mainly three different levels of image objects have been created representing different scales.

### 3.2.2 Second step: Classification

Classification is based on fuzzy logic. Each class of a classification scheme contains a class description. Each class description consists of a set of fuzzy expressions allowing the evaluation of specific features and their logical operation. A fuzzy rule can have one single condition or can consist of a combination of several conditions that have to be fulfilled for an object to be assigned to a class. The fuzzy sets were defined by membership functions that identify those values of a feature that are regarded as typical, less typical, or not typical of a class, i.e., they have a high, low, or zero membership respectively, of the fuzzy set.

The strategy for burned area classification was to create a three-level graded scale of segmentation. Thus, small object and larger objects would provide information about the final classification in level three. The reason for this approach was to build an operational model that would be easy to adapt to any LANDSAT TM data for burned area classification. Mainly three different levels of image objects representing different scales were created. At level 1, very small image objects were classified as the six different classes of confusion. They were then used for subsequent feature extraction. Large objects at level 3 were classified as “not burned”, “possibly burned” and “water”. After classifying level 3, a classification based fusion took place (Figure 4).

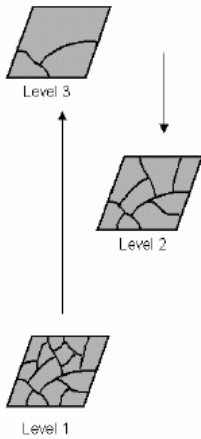


Figure 3: Different level of image segmentations

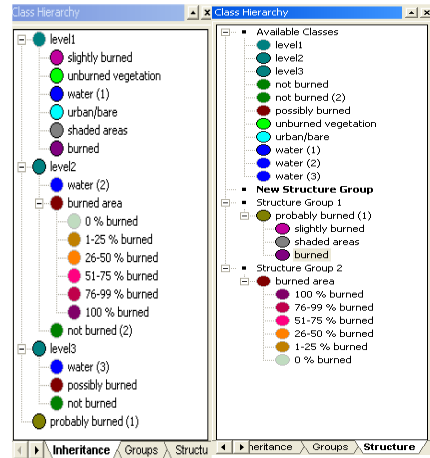


Figure 4: The first window shows the class hierarchy that contains all classification classes. The second window shows the structure hierarchy for classification-based segmentation

The principle of classification-based fusion is that all adjacent image objects that represent identical structures or are parts of identical structures are merged into one new image object. In this way, a number of image objects forming “burned area”, “slightly burned area” and “shaded areas” can be merged into one image object representing an entire “possibly burned area” (Figure 5). A structure is defined by organizing all classes that semantically form this structure in a “structure group”. Level 2 was the main classification level. First, “possibly burned” classified objects in level 3, and “slightly burned”, “shaded areas” and “burned” classified objects from level 1 were transferred to level 2. Secondly, a fuzzy rule base, using class related features, classifies all the objects at level 2.

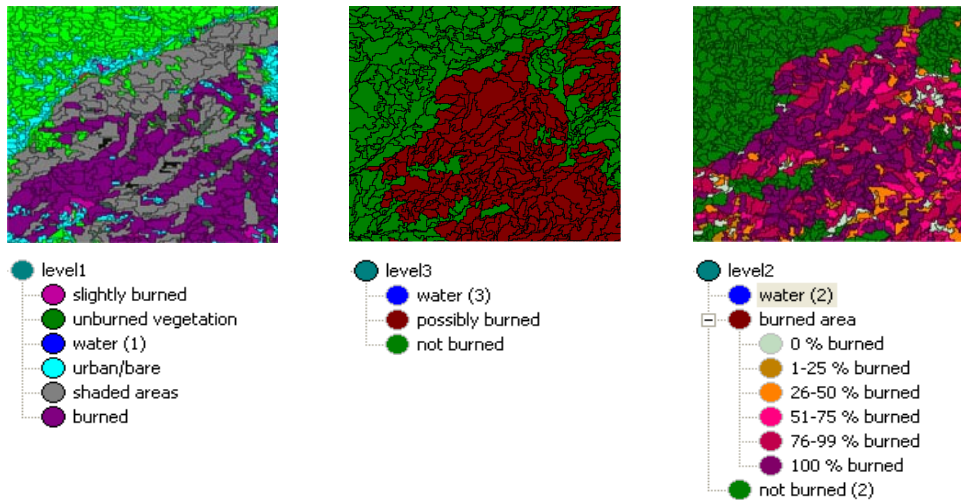


Figure 5: Subsets for the three different levels of classifications

Image regions of different textures were separated, even when they were of a similar spectral mean value, that make discriminating among different classes easier. Thus, confusions among different land cover types discussed in the first section could be easily eliminated by using contextual information. Note that the possibility of classification based segmentation obviously improved the classification result at the second level.

#### 4 CLASSIFICATION RESULTS AND DISCUSSIONS

It was necessary to obtain information about the classification stability and about how capable the classes were of extracting the desired image information. Besides the classical methods of accuracy assessment, special methods, based upon fuzzy concepts, were used. The classification results for the LANDSAT image were also compared to the fire perimeter map produced by the forest services of Greece and Spain (Figure 6).

Classification stability (Table 1) shows the difference between the best and the second best class assignment, calculated as a percentage. With this tool, it was possible to explore the differences in degrees of membership between the best and the second best class assignments of each object, thus removing the ambiguity regarding an object’s classification. The statistical output displays basic statistical operations (number of image objects, mean, standard deviation, minimum value and maximum value) performed on the best-to-second values per class. The classification stability table can be interpreted as follows: 2203 objects were classified as burned at level two; there was at least one object that belonged to another class other than “burned” with the same degree of membership

as the “burned” (minimum = 0.00). In general, the “burned” objects could definitely be separated from the other classes (mean =  $0.987 \pm 0.103$ ).

The classification confusion matrix or error matrix (Table 2) shows the commission and emission errors in the classification. The results of the object-oriented classification model showed that burned areas could be accurately mapped using LANDSAT TM data. The comparison of the classification with the burned area perimeter using 260 points is reported in table 2.

Of the 37 pixels that the logistic model predicted to be burned, only two pixels were erroneously classified as unburned. The overall classification accuracy was estimated to be 98.85%. The percentages of accuracy on the part of users and producers for burned area mapping were estimated to be 94.59% and 97.22% respectively. The landcover types confused with the burned areas were burned surfaces resulting from fires that took place in the previous year. It is interesting to note that due to topographic normalization and classifiers such as contextual features, the confusion between burned, shaded areas, water and urban was successfully eliminated.

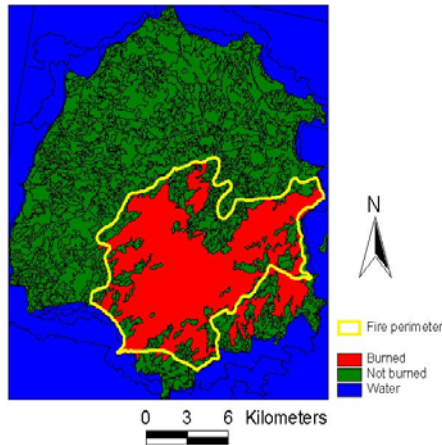


Figure 6: Burned area classification of the 1985 fire on Thasos, obtained by using the object-oriented model (the classified burned area beyond the yellow line is due to a recent previous fire)

Table 1. Classification stability (fuzzy accuracy assessment).

Classes	Objects	Mean	StdDev	Minimum	Maximum
Water	57	0.948486	0.147333	0.217241	1
Burned	2203	0.987	0.103	0	1
Not burned	728	0.99859	0.05593	0.041177	1

Table 2. Accuracy assessment for the final classification of the LANDSAT TM 1985

Classified data	Reference Data			Reference Totals	Classified Totals	Number Correct	Producers Accuracy	Users Accuracy
	W	B	NB					
Water (w)	90	0	0	90	90	90	100.00%	100.00%
Burned Areas (B)	0	35	2	36	37	35	97.22%	94.59%
Non-Burned Areas (NB)	0	1	132	134	133	132	98.51%	99.25%
Column Total	90	36	134	260	260	—	—	—
Overall Classification Accuracy = 98.85%								

#### 4.1 Accuracy and operationality assessment

Automation of the analysis process was achieved using two other LANDSAT datasets. All major steps in the classification process were included in a protocol file and were automatically applied to the images of the 19<sup>th</sup> September, 1989 from Greece and the 24<sup>th</sup> August, 1991 from Spain.

Cloud masking was carried out for the LANDSAT from Spain, using a ratio of channels 1 and 4 radiances (Figure 7). Clouds present high radiances in the visible band and very low radiances in the thermal channels, so the highest ratio values are closely related to cloud cover (Karteris 1992). By visual screening, a cloud threshold of ratio values was established in the image, and pixels within that range were to 0, and otherwise to 1. This cloud mask was multiplied by the original image scene for generating cloud free image. Afterwards, those masked areas within the fire perimeter generated by ICONA were assumed to be as burned lands in the LANDSAT image.

The burned area perimeters for the images of 1989 (Figure 8) and 1991 (Figure 9) produced by the Greek National Forest Service and ICONA, respectively, were used in the accuracy assessment of the two classifications.

In the classification stability analysis, the differences in degrees of membership between the best and the second best class assignments of each object were explored for the two images consecutively. For the LANDSAT of 1989, the objects of burned area could strongly be distinguished from other classes (mean  $0.994 \pm 0.0673$ ). Burned area classification accuracy assessment was also performed using error matrix. Producer's accuracy was found to be 94.87 %, while user's accuracy was 97.37%. The overall accuracy reached in this case study was 98.85%.

For the LANDSAT from Spain, the classified objects of burned area could strongly be distinguished from other classes (mean  $0.993 \pm 0.0812$ ). Burned area classification accuracy assessment was also performed using error matrix. Producer's accuracy was found to be 92.11 %, while user's accuracy was 97.22%. The overall accuracy reached in this case study was 98.46%.

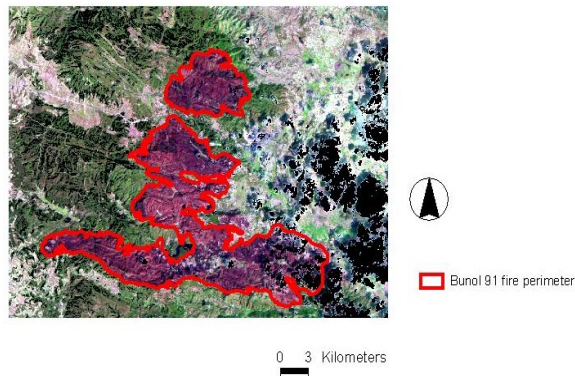


Figure 7: Cloud masking (in black) carried out for the LANDSAT (5-4-3) from Spain of the 24<sup>th</sup> August 1991 image, using a ratio of channels 1 and 4 radiances

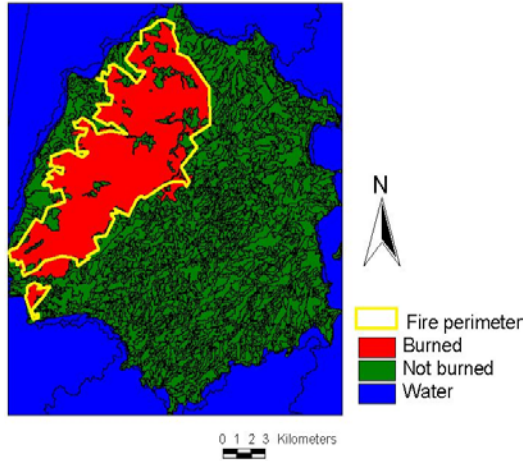


Figure 8: Burned area map of the 1989 fire obtained by applying an operational object-oriented model

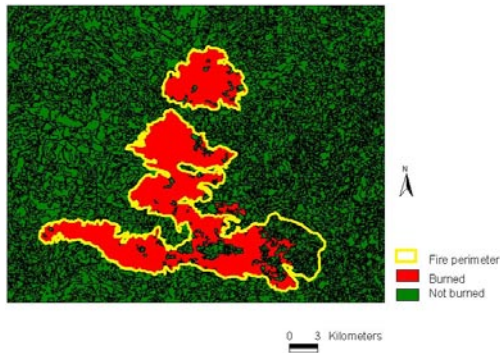


Figure 9: Burned area map of the 1991 fire obtained by applying an operational object-oriented model (refer to figure 7 for comparison)

## 5 CONCLUSIONS

The aim of this work was to develop an object-oriented classification model robust enough for operational burned area mapping in the Mediterranean ecosystems. In this study, a contextual algorithm for fire mapping using LANDSAT TM data was developed. Unlike “traditional” fire mapping algorithms applied to LANDSAT datasets (e.g. multi-channel thresholds), the model is self-adaptive, and is therefore a very consistent method for use in large areas, without the need to change the thresholds. The model was successfully applied in two different areas of the Mediterranean.

The main conclusion to be drawn from this work is that the classification process used in this study successively lead to very satisfactory results. The possibility of performing classification based segmentation obviously improved the classification result obtained at the second level. Fur-

thermore, the use of membership functions resulted in a reduction in the number of misclassified pixels. The combination of the new object-oriented image analysis approach (multi-resolution segmentation, hierarchical networks) with the multispectral high resolution data of LANDSAT TM showed very promising results. It constitutes an important step towards the integration of remote sensing and GIS, by providing operational means of interpretation high-resolution data.

Discriminating among the different confusion classes was possible using the contextual and spectral information supplied by the images. All steps involved in the image analysis could be recorded as a complete procedure. Thus, the whole strategy for solving a particular problem can be applied to other data of the same type. The main conclusions of this study can be summarized as follows:

- an object-oriented model was developed for mapping recently burned areas based on differentiation of the burned area from other classes of confusion;
- the model proved to be very accurate (approximately 96%) when tested in the case of the second fire that took place in a similar environment to that of the first;
- the model proved to be robust and operational when it was tested in a slightly different Mediterranean environment in Spain.

## ACKNOWLEDGEMENTS

The authors are grateful to Dr. Carlos Costa-Posada and Dr. Bernard Devereux, Unit for Landscape Modeling, University of Cambridge for their kind permission to use the DE\_RELIEF software. The authors are thankful to Dr. Emilio Chuvieco and Dr. David Riano, University of Alcalá for their generous contribution of the LANDSAT TM image from Spain.

## REFERENCES

- Alexandrian, D., 1995. Coastal Forest Reconstruction and Protection Project - Republic of Croatia, World Bank, Washington, DC.
- Baatz, M.A.S., 1999. Object-Oriented and Multi-Scale Image Analysis in Semantic Networks. In: Proc. of the 2nd International Symposium on Operationalization of Remote Sensing(Enschede. ITC).
- Baatz, M.A.S., 2000. Multiresolution segmentation - an optimization approach for high quality multi-scale image segmentation. *Angewandte Geographische Informationsverarbeitung XI. Beiträge zum AGIT-Symposium Salzburg 1999*. Karlsruhe, Herbert Wichmann Verlag.
- Caetano, M.S., Mertes, L.A.K. and Pereira, J.M.C., 1994. Using Spectral Mixture Analysis for Fire Severity Mapping, 2nd Int.Conf. Forest Fire Research, Coimbra, pp. 667-677.
- Caetano, M.S., Mertes, L., Cadete, L. and Pereira, J.M.C., 1996. Assessment of AVHRR data for characterising burned areas and post-fire vegetation recovery. *EARSeL Advances in Remote Sensing*, 4(4): 124-134.
- Calabri, G., 1986. *Prévention des incendies de forêts: information et éducation du public*, Valencia, Spain.
- Chuvieco, E. and Congalton, R.G., 1988. Mapping and inventory of forest fires from digital processing of TM data. *Geocarto International*, 4: 41-53.
- Chuvieco, E., 1997. Remote sensing applications in forest fires. In: P. Balabanis, G. Eftichidis and R. Fantechi (Editors), *Forest Fire Risk and Management*. Office for Official Publications of the European Communities, Luxembourg, pp. 193-207.
- Chuvieco, E., Deshayes, M., Stach, N., Cocero, D. and Riaño, D., 1999. Short-term fire risk: foliage moisture content estimation from satellite data. In: E. Chuvieco (Editor), *Remote Sensing of Large Wildfires in the European Mediterranean Basin*. Springer-Verlag, Berlin, pp. 17-38.
- Costa-Posada, C., 1997. *The Topographic Effect in Visible and Near Infrared Satellite Imagery*. PhD Thesis, University of Cambridge, Cambridge, UK, 199 pp.
- Díaz-Delgado, R., Salvador, R. and Pons, X., 1998. Monitoring of Plant Communities Regeneration after Fire by Remote Sensing. *International Journal of Wildland Fire*.
- Gitas, I.Z., 1999. *Geographical Information Systems and Remote Sensing in mapping and monitoring fire-altered forest landscapes*. PhD Dissertation Thesis, University of Cambridge, pp. 237

- Hofmann, T.P., J. & J. Buhmann, 1998. Unsupervised texture segmentation in a deterministic annealing framework. In: IEEE Transactions on Pattern Analysis and Machine Intelligence, Vol. 13: 478-482.
- ICONA, 1992. Los incendios forestales en España durante 1991, Instituto Nacional para la Conservación de la Naturaleza, MAPA, Madrid.
- Karteris, M.A., Meliadis, I.M., Kritikos, G.S. and Nikolaidis, A., 1992. Forest classification and mapping of Mediterranean forests and maquis with satellite data, Mediterranean Agronomic Institute of Chania, Chania, Greece.
- Lombraña, M.J., 1995. Monitoring of Burnt Forest Areas with Remote Sensing Data: A Study in North-East Spain using LANDSAT and SPOT XS Data. No. I.95.80, Institute for Remote Sensing Applications, Joint Research Centre, European Commission, Ispra, Italy.
- Makedos, I., 1987. The Pinus Brutia forest of Thasos. In: P. V., Pinus halepensis and Pinus Brutia forests (Ecology, management and development). Hellenic Association of Foresters, Chalkida, Greece, pp. 153-160.
- Milne, A.K., 1986. The use of remote sensing in mapping and monitoring vegetational change associated with bushfire events in Eastern Australia. *Geocarto International*, 1(1): 25-34.
- Minnaert, M., 1941. The reciprocity principle in Lunar photometry. *Astrophysical Journal*, 93(2): 403-410.
- Parnot, J., 1988. Inventaire des feux de brouse au Burkina Faso saison seche 1986-1987, 22nd International Symposium on Remote Sensing of the Environment. ERIM, Ann Arbor, Michigan, Abidjan, Cote d' Ivoire.
- Pereira, M.C. and Setzer, A.W., 1993. Spectral characteristics of fire scars in LANDSAT-5 TM images of Amazonia. *International Journal of Remote Sensing*, 14(11): 2061-2078.
- Pereira, J.M.C., Chuvieco, E., Beudoin, A. and Desbois, N., 1997. Remote Sensing of burned areas: a review. In: E. Chuvieco (Editor), A review of remote sensing methods for the study of large wildland fires. Departamento de Geografía, Universidad de Alcalá, Alcalá de Henares, pp. 127-184.
- Ponzoni, F.J., Lee, D.C.L. and Filho, P.H., 1986. Avaliacao da area queimada e da regeneracao da vegetacao afetada pelo fogo no Parque Nacional de Brasilia atraves de dados do TM/LANDSAT. In: R.S. Gramada (Editor), Simposio Latino-Americano de Sensoriamento Remoto, IV Simposio Brasileiro de Sensoriamento Remoto, INPE, Sao Jose dos Campos, Brazil.
- Richter, R., 1990. A Fast Atmospheric Correction Algorithm Applied To Landsat TM Images. *International Journal of Remote Sensing*, 11(1): 159-166.
- Rishmawi, K., 2001. Burned area and fire severity mapping on the Mediterranean island of Thasos using Landsat TM and Ikonos images, MAICH, Chania, 99-114 pp.
- Siljeström, P. and Moreno, A., 1995. Monitoring burnt areas by principal components analysis of multi-temporal TM data. *International Journal of Remote Sensing*, 16(9): 1577-1587.
- Silva, J.M.N., 1996. Comparacao entre os indices de vegetao NDVI e IV7 para cartografia de areas ardidas com imagens LANDSAT-5 TM, Instituto Superior de Agronomia, Universidade Tecnica de Lisboa, Lisbon.
- Simpson, C.J., 1990. Deep weathering, vegetation and fireburn. Significant obstacles for geoscience remote sensing in Australia. *International Journal of Remote Sensing*, 11(11): 2019-2034.
- Tanaka, S., Kimura, H. and Suga, Y., 1983. Preparation of a 1:25.000 LANDSAT map for assessment of burnt area on Etajima Island. *International Journal of Remote Sensing*, 4(1): 17-31.